NASA Technical Memorandum 106464
IEPC–93–098

Preliminary Far-Field Plume Sputtering Characterization of the Stationary Plasma Thruster (SPT–100)

Eric J. Pencil
Lewis Research Center
Cleveland, Ohio

Prepared for the
23rd International Electric Propulsion Conference
cosponsored by the AIAA, DGLR, AIDAA, and JSASS
Seattle, Washington, September 13–16, 1993

NASA

PRELIMINARY FAR-FIELD PLUME SPUTTERING CHARACTERIZATION OF THE STATIONARY PLASMA THRUSTER (SPT-100)

Eric J. Pencil*
National Aeronautics and Space Administration
Lewis Research Center
Cleveland, Ohio 44135

Abstract

For electric propulsion devices to be considered for use on communications satellites, integration impacts must be examined in detail. Two phenomena of concern associated with highly energetic plumes are contamination via sputtered material from the thruster and sputter erosion of downstream surfaces. In order to characterize the net effect of both phenomena, an array of witness plates were mounted in several types of holders and were exposed to the SPT-100 thruster plume for 50 hours. Surface analysis of the witness plates revealed that in the most energetic regions of the plume, there was a net removal of material from the samples facing the thruster. In the peripheral regions, net deposits were observed and characterized by the changes in optical properties of these samples. Changes in surface properties of samples located in collimators were within experimental uncertainty.

Nomenclature

$I(\lambda)$	solar spectral irradiance, W/(cm^2 μm)
R	radial distance downstream of thruster, m
R_s	ratio of energy reflected from sample to energy incident
R_{s+b}	measured reflectance or ratio of energy reflected from sample and plate system to energy incident
T_s	ratio of energy transmitted from sample to energy incident
α	absorptance from 350 to 1200 nm
ε_s	infrared emittance of sample
Θ	angular displacement from thruster centerline, degrees
λ	wavelength, nm
ρ	reflectance from 350 to 1200 nm
ρ_b	infrared reflectance of backing material
ρ_s	infrared reflectance of sample
$\rho(\lambda)$	spectral reflectance
τ	transmittance from 350 to 1200 nm
$\tau(\lambda)$	spectral transmittance
τ_s	infrared transmittance of sample

Introduction

The Stationary Plasma Thruster (SPT-100) is manufactured by Fakel Enterprises in Kaliningrad, Russia. This device uses an electrostatic field to accelerate ionized xenon to relatively high exit velocities. Recent interest in the application of the SPT-100 to commercial communications satellites has resulted from the reported performance levels associated with this device.[1,2] A program to more fully evaluate performance and characterize the plume of the SPT-100 is ongoing at NASA Lewis Research Center (LeRC).[3,4,5]

Application of any electric propulsion device for stationkeeping purposes raises concerns about the thruster plume impacts on spacecraft surfaces. Particle impacts by nonpropellant, neutral propellant, and ion beam effluxes can affect optical, thermal, and surface properties.[6] For example, degradation in the transmittance of translucent solar array cover slides would reduce the incident light reaching the solar cells, thereby lowering the solar array performance. Also, increasing absorptance or decreasing emittance result in higher solar cell operating temperatures, which degrade solar cell performance.

Previous work involving SPT devices investigated sputtering characteristics with an array of samples at a 1.0 meter distance from the thruster exit plane.[7] Many plasma properties, including mean ion energy were also investigated previously at a background pressure of 7×10^{-3} Pa (5×10^{-5} torr).[7] In that study, the mean ion energy was found to be maximum on the thruster centerline and to decrease to about 20% of the maximum at 60° off the centerline. Because sputter yield increases with increasing ion energy for samples at normal incidence, sputtering should be highest on centerline and decrease off axis.

Experiments detailed in this report were designed to examine degradation of representative materials due to SPT-100 plume impingement and deposition effects at a lower background pressure than was done previously. To quantify

* Aerospace Engineer, member AIAA.

sputtering effects, an array of quartz slides were positioned 2 m from the thruster exit plane. Both exposed witness plates and samples in collimators were used. The surface analyses used to characterize sputtering impacts included measurement of the change in sample mass. Optical and thermal properties measured were transmittance, absorptance, and emittance.

Apparatus and Procedure

Vacuum Facility

All experimental testing was performed in the 4.6 m diameter by 19.5 m long, stainless steel, vacuum facility shown in Figure 1. This facility had both diffusion pump and cryopump capabilities. The cryopumping system included one gaseous helium panel surrounded by two nitrogen panels. In order to minimize possible contamination by backstreaming diffusion pump oil, only the cryopump system was used. This system maintained an ambient pressure at the thruster of 7 x 10^{-4} Pa (5 x 10^{-6} torr) during thruster operation at a xenon flow rate of 5.4 mg/s.

Diagnostics

Quartz samples have been used previously in determining sputtering effects on solar cell cover slides.[8,9] For this study, 2 cm x 2 cm x 0.08 cm quartz slides were selected as test samples for the analysis of sputter degradation. The optically polished quartz samples had an RMS surface finish of 50 angstroms.

Masks of tantalum foil were used to cover portions of the exposed quartz slides as shown in Figure 2. The back of each quartz slide was also covered with foil to prevent contamination of this surface.

The collimators used a small aperture to limit the incident influx to the ion beam, as shown in Figure 3. The collimator diameter and length were 5 cm and 20 cm, respectively. The aperture in the cap facing the thruster was 3 mm in diameter. The quartz slide was positioned along the collimator centerline by a tantalum foil pocket.

Test Configuration

The Russian SPT-100 was mounted on a fixed stand and oriented coaxially with the vacuum facility. The distance from the thruster exit to a graphite-coated aluminum louver structure, shown in Figure 1, was about 8 m. An array of collimators and exposed cover slides were mounted on a rake at a radial distance of 2 m from the thruster exit as shown in Figure 4. This test was conducted simultaneously with a plume electrical characterization reported in detail elsewhere.[4] Exposed cover slides and collimators were located at 15° increments along the arc of the rake. Two exposed cover slides were located at each position. The vector normal to each sample pointed directly to the center of the thruster exit, such that the incident flow was approximately normal to all sample surfaces. The exposed surface of one sample faced towards the thruster, while the other faced away from the thruster. The two samples will be referred to in this report as front exposed and back exposed, respectively.

The thruster was operated with a power processing unit developed at LeRC and described elsewhere.[10] For the tests described in this report, the samples were exposed for 50 hours to the thruster operating under conditions listed in Table I.

Surface Analyses Instrumentation and Procedure

All masses in this report were measured with an electronic balance. Mass measurements were taken both before and after the 50 hour exposure. Repeatability was found to be ± 0.2 mg. The balance was enclosed in a plastic hood to prevent air circulation from affecting the readings.

Both transmittance and reflectance were measured with a spectrophotometer. This device contained a 60 mm barium sulfate coated integrating sphere used to compare the incident light intensity to the intensity of the light either transmitted through or reflected from a sample. The transmittance of each sample was measured directly, while the reported absorptance was calculated from the measured transmittance and reflectance. The measurement of the reflectance of a translucent material is sensitive to how the measurement is taken. The total reflectance of a translucent material is dependent on sample transmittance as well as the sample backing reflectance. The reflectance measurement of translucent materials requires the use of a sample backing which functions as a light trap, so that back reflectance is negligible. Due to the large number of samples, control samples were used as the baseline for the post-exposure measurements. The spectral response for all samples was measured from 350 to 1200 nm. Sample variance was determined to be 0.0013 from the transmittance measurements of 10 control samples.

The emittance of the samples was measured using an infrared reflectometer. This device measured the total room temperature emittance in the infrared spectrum using dual rotating cavities that sample radiation against a

room temperature blackbody. For this instrument, two different backings, with known infrared reflectance, were used to take two different reflectance measurements. Sample reflectance and transmittance were iteratively determined by solving the two resulting simultaneous equations. Due to the large number of samples, control samples were used as the baseline for post-exposure measurements. Sample variance was determined to be 0.003 from the emittance measurements of 10 control samples.

Results

Sample Mass

Figure 5 shows the change in mass of each sample resulting from the 50 hour exposure. For the front exposed samples there were two distinguishable regions of interest. In the region where $15^\circ \le \Theta \le 45^\circ$, there was a measurable loss in the mass of the samples. In the region where $60^\circ \le \Theta \le 90^\circ$, the changes in mass were within the uncertainty of the measurement. Most back exposed cover slides experienced a measurable net deposition. The exceptions were the slides at $\Theta = 60^\circ$ and 75°, whose weights remained the same. However, no consistent trends existed with respect to Θ for the back exposed samples. No significant changes in mass were observed with the collimator samples.

Transmittance

Spectral transmittance was measured over a wavelength range of 350 nm to 1200 nm. The spectral transmittance was approximately 0.93 for the unexposed control samples. The transmittance of the samples was calculated via equation 1 using a trapezoidal integration technique.

$$\tau = \frac{\int_{350\,nm}^{1200\,nm} \tau(\lambda) I(\lambda) d\lambda}{\int_{350\,nm}^{1200\,nm} I(\lambda) d\lambda} \qquad (1)$$

Figure 6 shows the total transmittance as a function of angular displacement from the thruster centerline. It should be noted that the uncertainty bars for transmittance were smaller than the plot symbols used in Figure 6. In the case of the front exposed sample at $\Theta = 15^\circ$, some tantalum foil had inadvertently pulled away from the back of the witness plate, thereby unmasking portions of the back surface. Because the transmittance was measured over approximately 1 cm^2 area of the sample, an accurate measurement was not possible for this specimen. The transmittance for the front exposed samples in the region of $30^\circ \le \Theta \le 60^\circ$ did not change significantly from that of the baseline 0.93. In the region of $60^\circ \le \Theta \le 90^\circ$, a measurable change in sample transmittance occurred, with the transmittance decreasing for increasing Θ. As shown in Figure 6, the degradation of transmittance for the back exposed samples, due to tank wall material, decreased for the entire array of samples with the maximum decrease occurring near the centerline. No significant change in transmittance was measured for any of the collimator cover slides.

Absorptance

The spectral reflectance was approximately 0.07 for the unexposed control samples. Using a trapezoidal integration technique, the reflectance was calculated as:

$$\rho = \frac{\int_{350\,nm}^{1200\,nm} \rho(\lambda) I(\lambda) d\lambda}{\int_{350\,nm}^{1200\,nm} I(\lambda) d\lambda} \qquad (2)$$

Absorptance for a translucent material was then calculated from reflectance and transmittance as:

$$\alpha = 1 - \tau - \rho \qquad (3)$$

Figure 7 shows the absorptance of the samples after the 50 hour exposure to the thruster plume. Uncertainty bars for this measurement were again smaller than the plot symbols. Typical absorptance for unexposed control samples was approximately 0.0. The absorptance of the sample at $\Theta = 15^\circ$ had an artificial increase in absorptance due the poor transmittance measurement described earlier. No measurable change in absorptance was observed in the front exposed samples between $30^\circ \le \Theta \le 60^\circ$. In the region for $60^\circ \le \Theta \le 90^\circ$, a measurable change in the absorptance was observed, with the absorptance increased with increasing Θ. A measureable increase in absorptance occurred for all back exposed samples, with the change in absorptance increasing with increasing Θ. Changes in the absorptance of the samples located in the collimators were within experimental uncertainty.

An accuracy limitation of the spectrophotometer was discovered by the consistent measurement of negative absorptances for translucent materials. Measurements of the control samples, the collimator samples, and the front exposed samples for $30^\circ \le \Theta \le 60^\circ$, showed that all had slightly negative absorptances. This systematic error was likely due to an overestimated reflectance. The reflectance of the backing material, functioning as a light trap, was

found to be approximately 0.003 when integrated from 350 to 1200 nm. With this correction the absorptance of these samples fell within random experimental uncertainty of the baseline of 0.0 rather than -0.003.

Emittance

The reflectance of a translucent sample with an opaque backing was related to the sample and backing properties by the following set of equations:[11]

$$R_{s+b} = R_s + \frac{\rho_b T_s^2}{1-\rho_b R_s} \quad (4)$$

$$R_s = \rho_s\left[1+\frac{(1-\rho_s)^2\tau_s^2}{(1-\rho_s^2\tau_s^2)}\right] \quad (5)$$

$$T_s = \frac{\tau_s(1-\rho_s)^2}{(1-\rho_s^2\tau_s^2)} \quad (6)$$

By measuring the reflectance with two different backings, both the sample transmittance and reflectance were obtained iteratively. It was found that typical transmittance for the unexposed control samples were 7 - 8%, which agreed with a typical quartz transmittance of 0.1 at 4 μm.[12] The sample reflectance was measured using a backing material with a low infrared reflectance of 0.089. Since the samples were nearly opaque, the infrared emittance was approximated by the following equation

$$\varepsilon_s = 1-\rho_s \quad (7)$$

Typical emittances for the unexposed control samples were 0.82, which compared to the total emittance of quartz of 0.9.[13]

Figure 8 shows the angular distribution of the infrared emittance of the samples after the 50 hour exposure. Uncertainty bars for this figure were smaller than the plot symbols. The emittance of all the front exposed samples did not change within the experimental uncertainty. For the back exposed samples in the region of $15^\circ \le \Theta \le 45^\circ$, there were measurable decreases in emittance, with the maximum change occurring closest to the centerline. For the back exposed samples in the region of $60^\circ \le \Theta \le 90^\circ$, the changes in emittance were within experimental uncertainty. None of the collimator samples experienced a measurable change in emittance within experimental uncertainty.

Discussion of the Results

Front exposed samples

In the region between $15^\circ \le \Theta \le 45^\circ$, net erosion occurred, based on the mass losses in Figure 5. Sample erosion varied significantly with angle. The mass loss of the quartz slide at 45° was about 7% of the erosion at 15° with respect to the thruster centerline. All other changes in properties were within experimental uncertainty. This leads to two conclusions. First, the cleaning action of the higher energy ions in this region[7] removed any tank wall material that was deposited. Second, the transmittance, absorptance, and emittance of the samples did not decrease even though material was being eroded from the surface. This was not unexpected as previous work has shown that quartz samples, when exposed to a 3 keV mercury ion flux, had negligible change in absorptance or emittance.[14]

For the sample at $\Theta = 60^\circ$, all changes in sample properties were within experimental error.

For the samples in the region where $75^\circ \le \Theta \le 90^\circ$, change in transmittance and absorptance indicated that a net deposit of thruster material and/or tank wall material occurred. The change in both the sample mass and emittance were within experimental uncertainty. The change in transmittance and absorptance increased as the angle relative to the thruster centerline increased. This observed trend can be explained by the combination of two effects. The samples in the peripheral regions viewed larger sources of sputtered efflux from the downstream regions of the vacuum facility. Also, the lower mean ion energy in the peripheral regions of the plume resulted in lower sputter yields. Sputter yields approach zero for ion energies below 50 eV.[15] This lower sputter yield resulted in less material being removed from these samples. It should be noted that the deposition effects in space should be very different because there would be no contaminating facility material.

Back exposed samples

For the samples in the region where $15^\circ \le \Theta \le 45^\circ$, all measurements indicated that a net deposit of tank material occurred. There were no consistent trends for the mass and transmittance measurements as a function of Θ in this region. The largest changes in absorptance and emittance occurred closer to the thruster centerline. This trend indicated that the optical densities of films sputtered from the facility were significantly higher in this region.

For the samples in the region where $60^\circ \leq \Theta \leq 90^\circ$, the change in transmittance and absorptance indicated that a net deposition of tank wall material occurred. The changes decreased with increasing Θ, which was a continuation of the trend from the centerline. The changes in mass and emittance for these samples were within experimental error.

Collimator samples

No measurable change in any sample property occurred with any collimator sample. Collimator samples were exposed to a limited influx from the thruster by the small aperture. The ratio of aperture area to exposed cover slide area was about 1:40. Thus the expected deposition would be a fraction of that measured on the front exposed slides which would be within the measurement experimental uncertainty. In order to obtain measurable results with collimator samples, it will be necessary to increase the aperture diameter and/or exposure times, and/or reduce radial distance from the samples to the thruster.

Conclusions

In order to assess the impacts of the SPT-100 sputtering on spacecraft subsystems, an array of quartz witness plates was positioned at a radial distance of 2 meters downstream of the thruster exit plane and exposed to the thruster plume for 50 hours. Several sputtering phenomena were investigated simultaneously. These included sputtering of material from the thruster to the witness plates, sputtering of material from the tank wall to the witness plates, and sputtering of material from the witness plates. Both front and back exposed slides and quartz samples mounted in collimators were used in this experiment. Collimation was chosen to eliminate sample contamination by backsputtered material from the facility. The net erosion or net deposition was examined by measuring the change in mass of the samples. Changes in thermal and optical properties (transmittance, absorptance, and emittance) were also measured to determine the impact of contamination on the performance of a solar array. General trends common to most measurements were the net deposit of materials in the peripheral regions of the plume for samples facing towards the thruster, either characterized by increasing mass or changes in optical properties. The samples located at angles closer to the centerline than 60 degrees were apparently not contaminated by wall material due to cleaning by the ion beam. The back exposed samples nearest the thruster centerline incurred the largest change in optical properties, due to sputtered efflux from the facility. No measurable changes in surface properties occurred for the collimator samples. In order to obtain measurable results with collimator samples, future tests will require increased exposure time and/or aperture diameter, and/or reduced radial distance. These preliminary experiments will help define detailed requirements for more extensive tests which will assess plume impacts on spactraft materials located downstream of electric thrusters.

References

1. Bober, A.S., *et al.*, "State of Work on Electrical Thrusters in USSR," Proceedings of the 22nd International Electric Propulsion Conference, Viareggio, Italy, October 1991.

2. Brophy, J.R., *et al.*, "Performance of the Stationary Plasma Thruster: SPT-100," AIAA 92-3155, July 1992.

3. Sankovic, J.M., Hamley, J.A., and Haag, T.W., "Performance Evaluation of the Russian SPT-100 Thruster at NASA LeRC," IEPC 93-094, Proceedings of the 23rd International Electric Propulsion Conference, September 1993, to be published.

4. Myers, R.M. and Manzella, D.H., "Stationary Plasma Thruster Plume Characteristics," IEPC 93-096, Proceedings of the 23rd International Electric Propulsion Conference, September 1993, to be published.

5. Manzella, D.H., "Stationary Plasma Thruster Plume Emissions," IEPC 93-097, Proceedings of the 23rd International Electric Propulsion Conference, September 1993, to be published.

6. Byers, D.C., "Electron Bombardment Thruster Field and Particle Interfaces," Journal of Spacecraft and Rockets, Vol. 16, No. 5, pp 289-301, September-October, 1979.

7. Absalamov, S.K., *et al.*, "Measurement of Plasma Parameters in the Stationary Plasma Thruster (SPT-100) Plume and Its Effect on Spacecraft Components," AIAA 92-3156, July 1992.

8. Reynolds, T.W. and Richley, E.A., "Contamination of Spacecraft Surfaces Downstream of a Kaufman Thruster," NASA TN D-7038, January 1971.

9. Weigand, A.J. and Mirtich, M.J., "Change in Transmittance of Fused Silica as a Means of Detecting Material Sputtered from Components on a 5-cm Ion Thruster," NASA TMX-68073, May 1972.

10. Hamley, J.A., Hill, G., and Sankovic, J.M., "Power Electronics Development for the SPT-100 Thruster," IEPC-93-044, Proceedings of the 23rd International Electric Propulsion Conference, September 1993, to be published.

11. Siegel, R. and Howell, J.R., Thermal Radiation Heat Transfer, Second Edition, Hemisphere Publishing Corp., New York, 1981.

12. Smith, W.J., Modern Optical Engineering, The Design of Optical Systems, McGraw-Hill Book Co., New York, 1966.

13. Holman, J.P., Heat Transfer, Sixth Edition, McGraw-Hill Book Co., New York, 1986.

14. Hall, D.F. and Kelley, L.R., "Experimental Techniques to Determine Electrostatic Rocket Exhaust Effects on Spacecraft Surfaces," AIAA 70-1144, September 1970.

15. Rosenburg, D. and Wehner, G.K., "Sputtering Yields for Low Energy Ion Bombardment," Journal of Applied Physics, Vol. 33, No. 5, pp 1842-1845, May 1962.

Table I - SPT-100 operating conditions.

Discharge voltage	300 V
Discharge current	4.5 A
Xenon total mass flow rate	5.4 mg/s
Ratio of anode to cathode mass flow rates	19

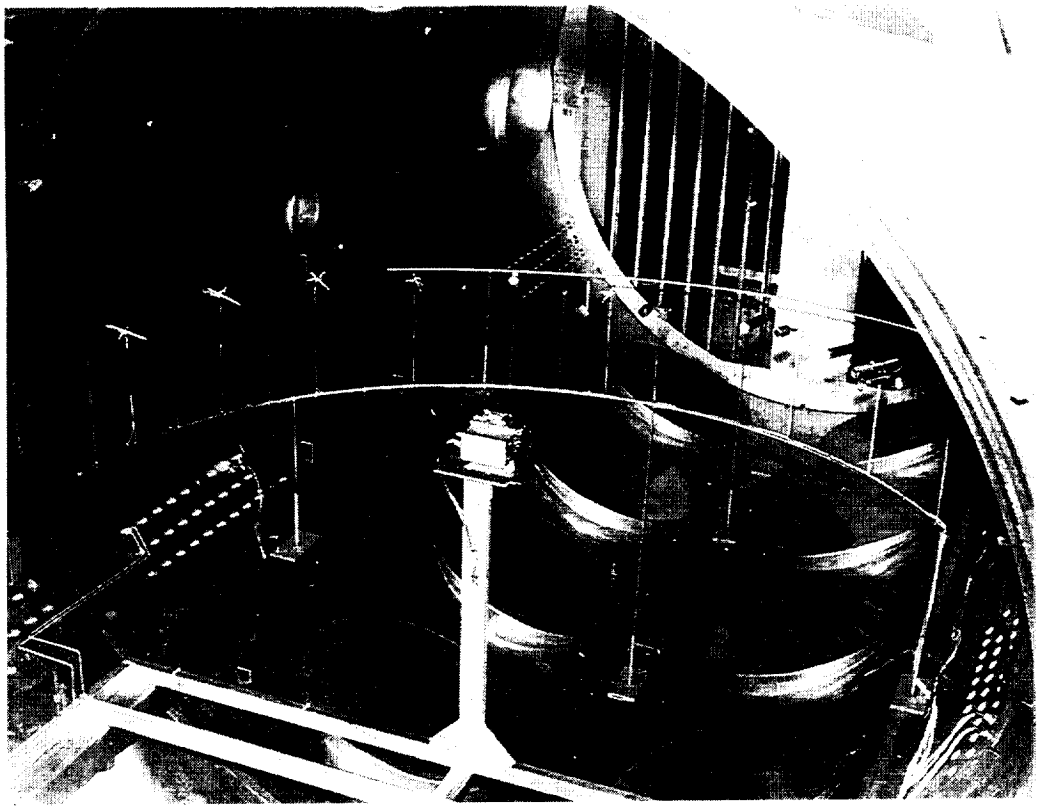

Figure 1 - View of 4.6 m diameter vacuum facility with experimental setup.

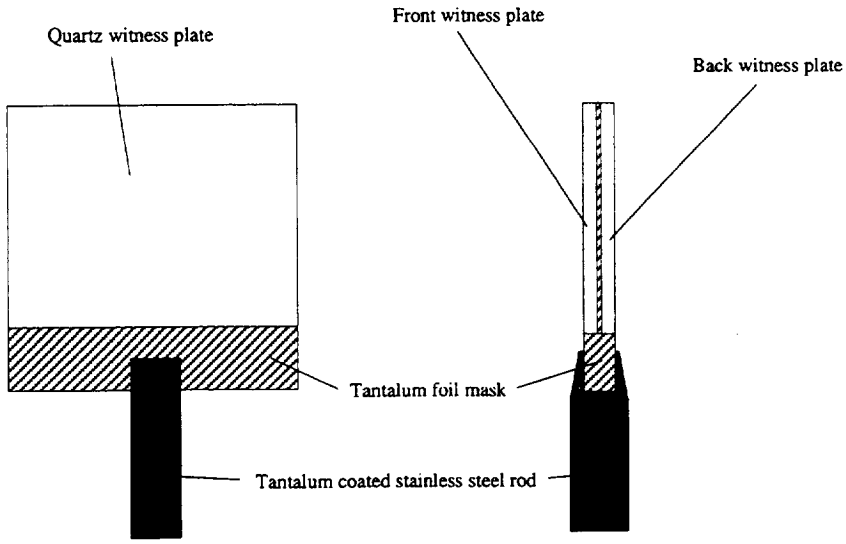

Figure 2 - Schematic of exposed cover slide holder.

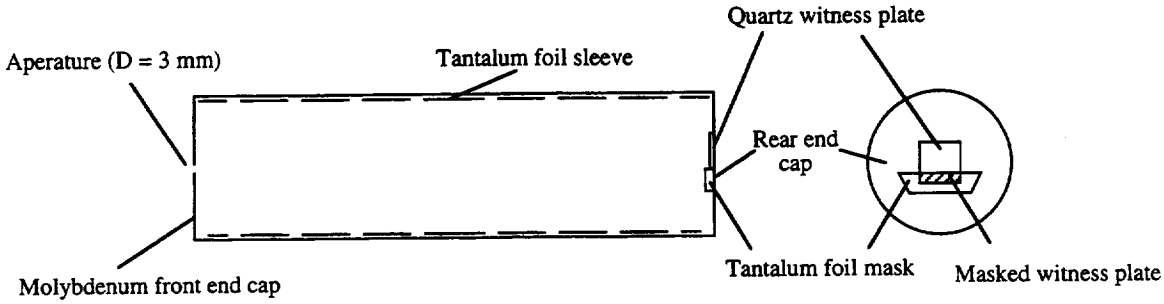

Figure 3 - Schematic of collimator and sample holder.

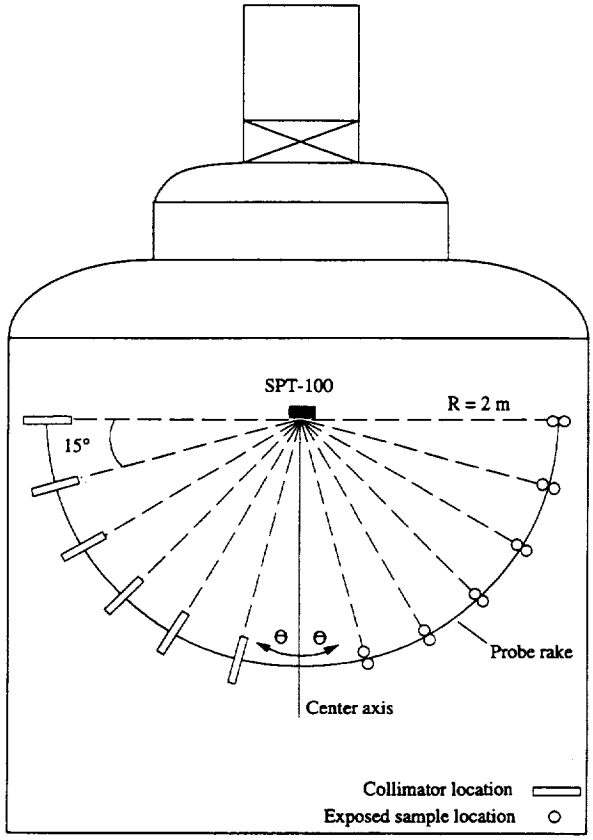

Figure 4 - Schematic of far-field plume probe locations, top view of facility.

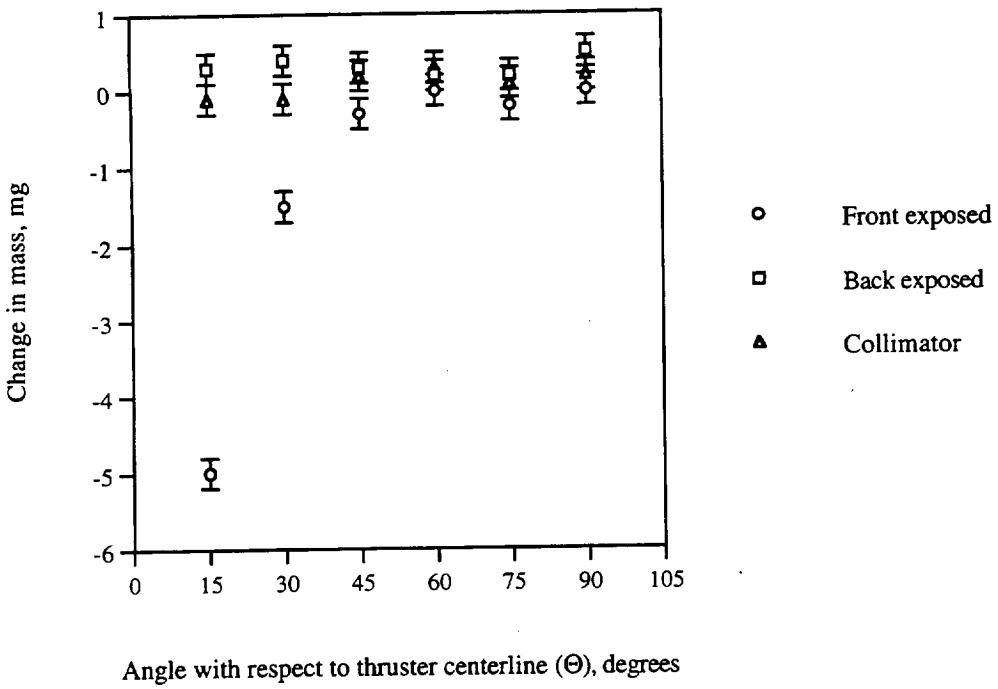

Figure 5 - Change in mass of quartz witness plates after 50 hour exposure.

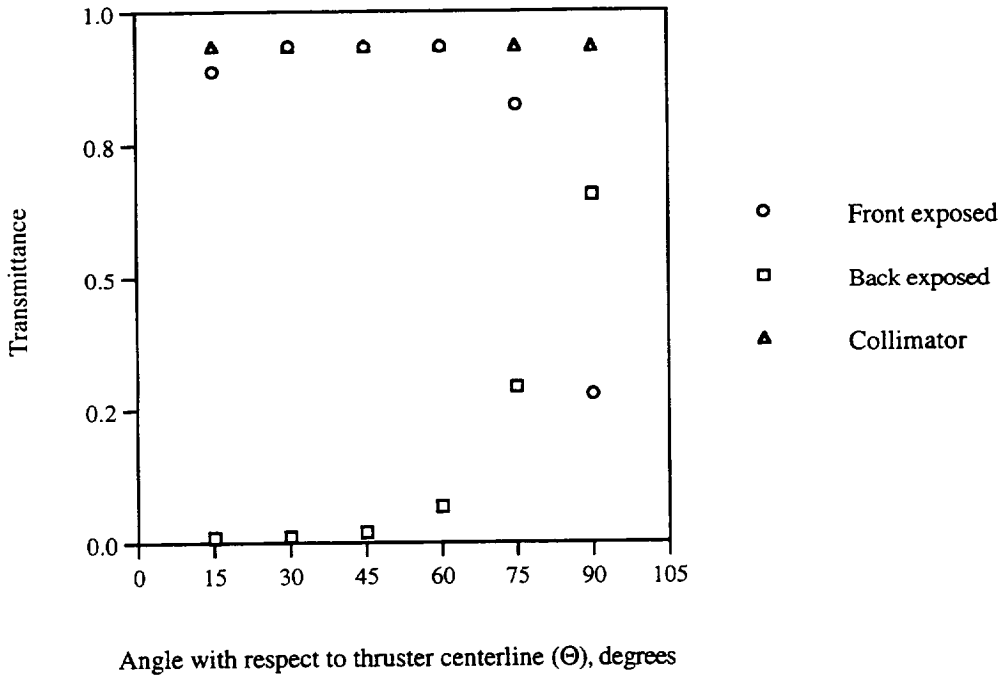

Figure 6 - Transmittance of witness plates after 50 hour exposure.

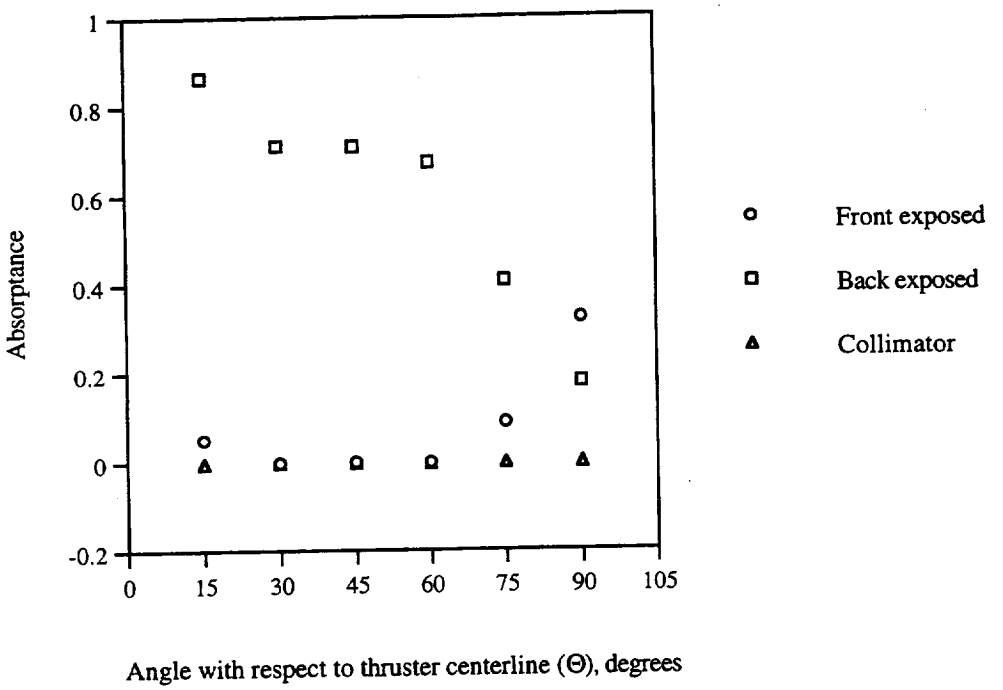

Figure 7 - Absorptance of witness plates after 50 hour exposure.

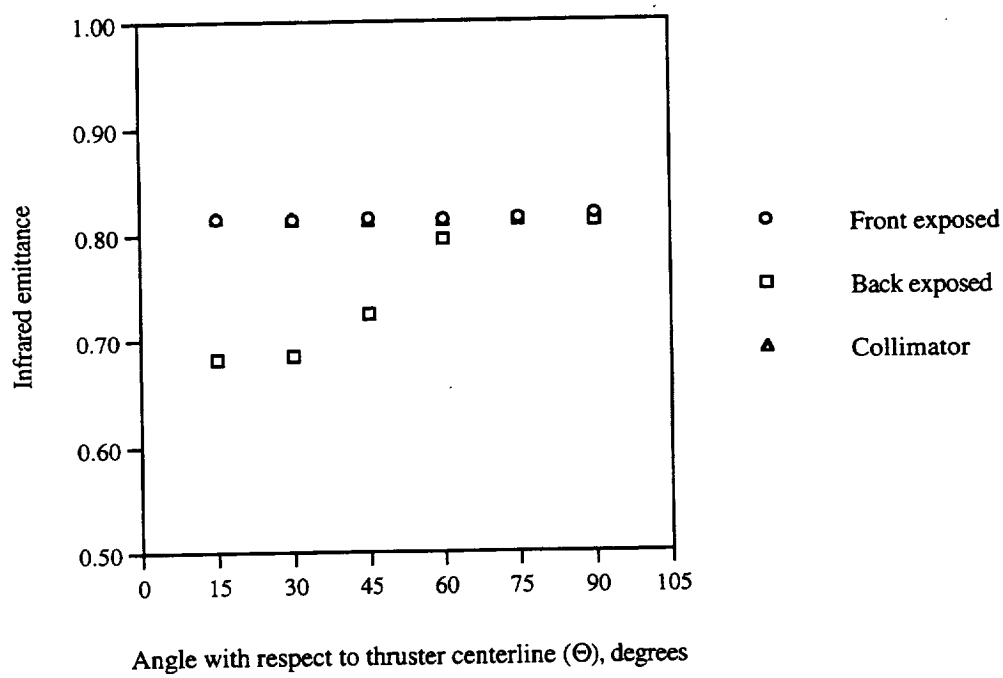

Figure 8 - Infrared emittance, at 25°C, of witness plates after 50 hour exposure.

REPORT DOCUMENTATION PAGE

Form Approved
OMB No. 0704-0188

1. AGENCY USE ONLY (*Leave blank*)	2. REPORT DATE	3. REPORT TYPE AND DATES COVERED
	January 1994	Technical Memorandum

4. TITLE AND SUBTITLE

Preliminary Far-Field Plume Sputtering Characterization of the Stationary Plasma Thruster (SPT–100)

5. FUNDING NUMBERS

WU–506–42–31

6. AUTHOR(S)

Eric J. Pencil

7. PERFORMING ORGANIZATION NAME(S) AND ADDRESS(ES)

National Aeronautics and Space Administration
Lewis Research Center
Cleveland, Ohio 44135–3191

8. PERFORMING ORGANIZATION REPORT NUMBER

E–8328

9. SPONSORING/MONITORING AGENCY NAME(S) AND ADDRESS(ES)

National Aeronautics and Space Administration
Washington, D.C. 20546–0001

10. SPONSORING/MONITORING AGENCY REPORT NUMBER

NASA TM–106464
IEPC–93–098

11. SUPPLEMENTARY NOTES

Prepared for the 23rd International Electric Propulsion Conference cosponsored by the AIAA, DGLR, AIDAA, and JSASS, Seattle, Washington, September 13–16, 1993. Responsible person, Eric J. Pencil, (216) 433–7463.

12a. DISTRIBUTION/AVAILABILITY STATEMENT

Unclassified - Unlimited
Subject Category 20

12b. DISTRIBUTION CODE

13. ABSTRACT ***(Maximum 200 words)***

For electric propulsion devices to be considered for use on communications satellites, integration impacts must be examined in detail. Two phenomena of concern associated with highly energetic plumes are contamination via sputtered material from the thruster and sputter erosion of downstream surfaces. In order to characterize the net effect of both phenomena, an array of witness plates were mounted in several types of holders and were exposed to the SPT-100 thruster plume for 50 hours. Surface analysis of the witness plates revealed that in the most energetic regions of the plume, there was a net removal of material from the samples facing the thruster. In the peripheral regions, net deposits were observed and characterized by the changes in optical properties of these samples. Changes in surface properties of samples located in collimators were within experimental uncertainty.

14. SUBJECT TERMS

Collimator; Sputtering; Hall effect thruster; Integration testing; Electric propulsion

15. NUMBER OF PAGES
12

16. PRICE CODE
A03

17. SECURITY CLASSIFICATION OF REPORT	18. SECURITY CLASSIFICATION OF THIS PAGE	19. SECURITY CLASSIFICATION OF ABSTRACT	20. LIMITATION OF ABSTRACT
Unclassified	Unclassified	Unclassified	